

Magnetic Neutron Scattering from Atoms Dissolved in Ferromagnetic Iron and Nickel

G. G. Low

Citation: [Journal of Applied Physics](#) **39**, 1174 (1968); doi: 10.1063/1.1656216

View online: <http://dx.doi.org/10.1063/1.1656216>

View Table of Contents: <http://scitation.aip.org/content/aip/journal/jap/39/2?ver=pdfcov>

Published by the [AIP Publishing](#)

Articles you may be interested in


[Neutron Emission Spectra from Inelastic Scattering on \$^{58,60}\text{Ni}\$ with a White Neutron Source at FIGARO](#)
AIP Conf. Proc. **769**, 985 (2005); 10.1063/1.1945170

[Above-room-temperature ferromagnetic \$\text{Ni}^{2+}\$ -doped ZnO thin films prepared from colloidal diluted magnetic semiconductor quantum dots](#)
Appl. Phys. Lett. **85**, 1395 (2004); 10.1063/1.1785872

[Comparison of Electron Elastic-Scattering Cross Sections Calculated from Two Commonly Used Atomic Potentials](#)
J. Phys. Chem. Ref. Data **33**, 409 (2004); 10.1063/1.1595653

[Extraction of Neutron Density Distributions from Proton Elastic Scattering at Intermediate Energies](#)
AIP Conf. Proc. **675**, 720 (2003); 10.1063/1.1607229

[Magnetic resistivity and electron–magnon scattering in 3d ferromagnets](#)
J. Appl. Phys. **91**, 8129 (2002); 10.1063/1.1456434


 **SHIMADZU**
Excellence in Science

Powerful, Multi-functional UV-Vis-NIR and FTIR Spectrophotometers

Providing the utmost in sensitivity, accuracy and resolution for applications in materials characterization and nano research

- Photovoltaics
- Polymers
- Thin films
- Paints
- Ceramics
- DNA film structures
- Coatings
- Packaging materials

[Click here to learn more](#)



Magnetic Neutron Scattering from Atoms Dissolved in Ferromagnetic Iron and Nickel

G. G. Low

Atomic Energy Research Establishment, Harwell, Berkshire, England

Recent experimental results giving the distribution of the magnetic-moment disturbance associated with solute atoms in ferromagnetic iron and nickel are summarized. The disturbances around transition elements dissolved in iron are of two quite different forms dependent on whether the element concerned lies to the right or to the left of iron in the periodic table. This suggests a dependence on the sign of an electrostatic perturbing potential and a discussion of this possibility is given in terms of a simple electron gas model. The two types of magnetic disturbance observed are not related by a sign reversal and the nonlinearity thus demanded by experiment is thought to result from limitations on electron-density increases imposed in iron by the restricted number of orbitals available at any one site. Experimental results for iron alloys containing nontransition-element solutes are also examined. Measurements on a wide range of both transition and nontransition elements dissolved in nickel are reviewed. Zn, Al, Ga, Si, Ge, Sn, Sb, V, Cr, Nb, Mo, Ru, W, and Re all result in a widespread loss of magnetic moment from the nickel host surrounding a solute site. The magnetic disturbances corresponding to these impurities differ in magnitude but show an approximately invariant shape. These defects are discussed in terms of bound impurity states and a molecular-field treatment involving a nonlocal and nonlinear susceptibility to represent the magnetic properties of nickel.

1. INTRODUCTION

This paper contains a summary of the recent neutron-scattering work concerning the distribution of magnetization at impurity atoms dissolved in ferromagnetic iron and nickel. The interpretation of the experimental data is discussed with the aid of models to represent the properties of the iron and nickel matrices. These models incorporate in a crude way the results of recent band-theory calculations, and the discussion therefore goes some distance towards relating the behavior of iron- and nickel-based alloys to the properties of the host materials.

The details of the experimental method have been given previously.¹ The elastic magnetic diffuse scattering of neutrons is related to the disturbance in magnetic moment density, $\rho'(\mathbf{r})$, associated with a single impurity atom at $\mathbf{r}=0$ by the differential cross section

$$d\sigma/d\Omega = (\gamma e^2/2mc^2)^2 \sin^2\alpha \left| \int d\mathbf{r} \rho'(\mathbf{r}) \exp(i\mathbf{k}\cdot\mathbf{r}) \right|^2. \quad (1)$$

κ is the neutron-scattering vector ($\kappa = 4\pi \sin\theta/\lambda$, where θ is half the scattering angle) and α is the angle between κ and the direction of magnetization of the sample. The integral is over the volume of the sample. This expression may be inverted to give $\rho'(\mathbf{r})$ in terms of $d\sigma/d\Omega$. The plots of $\rho'(\mathbf{r})$ so obtained are the starting point of the present discussions. Details of the inversion process can be found in the experimental papers. The published results all refer to polycrystalline specimens and consequently the $\rho'(\mathbf{r})$ curves represent a spherical average. However, unpublished work on a few single-crystal specimens shows only small anisotropy effects of magnitude similar to the experimental errors and thus the polycrystalline sample results appear to provide a reasonably accurate representation of the actual

physical situation. In any case it must also be borne in mind that the experiments are inherently of rather low resolving power and that averaging over a resolution width, i.e., over some 2 Å, is always present.

2. IRON-BASED ALLOYS

A. Transition-Element Solutes

The scattering from dilute concentrations of 15 transition-element impurities in iron has been measured by Collins and Low.² All the scattering data fall into one of two patterns apart from the cases of Ti and Mn which therefore require separate discussion.^{2,3} This can be seen in Fig. 1 where the scattering amplitudes corresponding to the magnetic-moment disturbance in the matrix around a solute site are plotted for the other 13 impurities as a function of scattering vector. The two patterns observed in the scattering data correspond on the one hand to elements to the right of iron in the periodic table (Co, Ni, Rh, Pd, Ir, Pt) and on the other to elements to the left of or under iron (Cr, V, Ru, Mo, Os, Re, W). Sketches of the magnetic moment density disturbances around impurity sites for these two cases are shown in Fig. 2.

On the whole, the dilute alloys of iron roughly follow a Slater-Pauling curve behavior. Thus, if we adopt a simple band picture, it would appear that screening around a perturbing charge is dominated by majority spin carriers. This is confirmed by the self-consistent band-theory calculations for iron of Wakoh and Yamashita⁴ which give a high density of states at the

² M. F. Collins and G. G. Low, *Proc. Phys. Soc. (London)* **86**, 535 (1965). See also I. A. Campbell, *Proc. Phys. Soc. (London)* **89**, 71 (1966) for an alternative method of analyzing the experimental scattering data.

³ G. G. Low, *Phys. Letters* **21**, 497 (1966).

⁴ S. Wakoh and J. Yamashita, *J. Phys. Soc. Japan* **21**, 1712 (1966).

¹ G. G. Low and M. F. Collins, *J. Appl. Phys.* **34**, 1195 (1963).

Fermi level for the majority spin direction. The origin of the magnetic moment changes at impurities which come from the left of iron in the periodic table therefore seems to be straightforward. On this simple model, the reduction in core charge (Δz negative) at the impurity site repels electrons mostly from the majority spin bands. There is, therefore, a considerable loss of moment from the impurity cell, in qualitative agreement with observation.² No doubt other processes, including perhaps the formation in some instances of bound states⁵ and variations in exchange effects, are of importance in any quantitative discussion. However, qualitatively the situation appears to be in accordance with the simple picture above.

If we now turn to the solutes which come from the right of iron in the periodic table the simple mechanism described does not produce effects bearing even a rough qualitative correspondence with the experimental facts. The change in core charge Δz is now positive and, from the above process, a positive magnetic-moment disturbance would be expected in the impurity cell. Experiment² shows losses of moment of between $\frac{1}{2}$ and $2 \mu_B$.

The physical reason underlying this nonlinearity in behavior as a function of core charge is thought to be connected with the small number of holes in the majority spin bands in iron. It appears from the density of states plots given by Wakoh and Yamashita that an increase in majority spin electron population of only 0.15 per atom reduces the density of states at the Fermi level corresponding to this spin direction to a very low level. Thus, the majority spin bands will become ineffective in the screening of attractive charges beyond this point and further screening must be provided almost entirely by minority spin carriers.

As the screening charge is piled up locally around an impurity, saturation of screening capability in this way

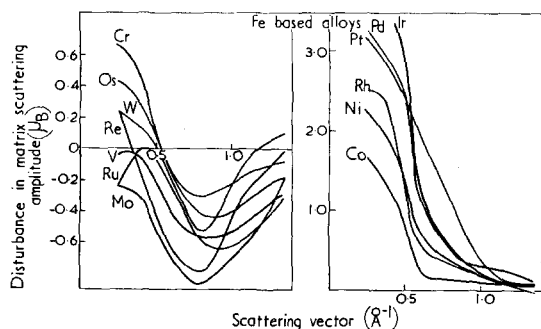


FIG. 1. Defect scattering amplitudes associated with the iron matrix surrounding transition-element solute atoms. Two distinct patterns are found depending on whether the solute lies to the right of iron in the periodic table or on the other hand to the left of or under iron. These curves are based on the neutron-scattering experiments of Collins and Low.²

⁵ I. A. Campbell and A. A. Gomès, Proc. Phys. Soc. (London) **91**, 319 (1967).

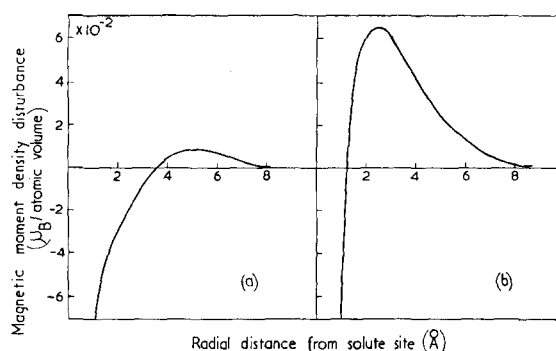


FIG. 2. Sketches of the disturbances in magnetic-moment density associated with transition-element solutes in iron: (a) elements to the left of iron in the periodic table and (b) elements to the right of iron. In both cases there are considerable losses of magnetic moment from the impurity cell. (The nearest-neighbor distance for Fe is 2.5 Å.)

can occur at an individual solute site in a dilute alloy. In other words the electrons involved in the screening must physically reside in the atomic orbitals which go to make up the majority carrier bands and if these are almost full already in pure iron, only a very small increment in charge can be brought to bear in the impurity cell where it is required. If the majority carriers are ineffective in this way in the screening of attractive core-charge changes, the minority carrier d band will of necessity provide the required screening. Now, however, we expect a decrease in magnetic moment to ensue from the screening process. Thus, with regard to changes in the impurity cell, we now have agreement with the trend of the moment losses observed experimentally.²

Outside the impurity cell, i.e., at the nearest-neighbor positions, only a relatively small amount of screening per atomic volume, which is largely within the capability of the few holes in the majority carrier bands, is demanded. Thus, an increase in magnetic moment at iron atoms neighboring an impurity of positive Δz is expected. This is again in accord with experiment as can be seen from Fig. 2(b). It appears that this contribution to the total magnetic-moment change outweighs the loss in the impurity cell itself and thus leads to a positive value for $d\bar{\mu}/dc$, the rate of change of net magnetic moment with concentration, and a rough Slater-Pauling like behavior. In fact $d\bar{\mu}/dc$ for small additions of elements to the right of iron in the periodic table is in general less than $-d\bar{\mu}/dc$ for elements a corresponding number of columns to the left of iron. This can now be seen to be the consequence of the saturation effect in the screening of attractive charge.

The ideas outlined above have been incorporated in a crude model in which three electron gases are used to represent the properties of the iron matrix.⁶ Each gas is characterized in terms of a density of states and a

⁶ G. G. Low, Proc. Phys. Soc. (London) **92**, 938 (1967).

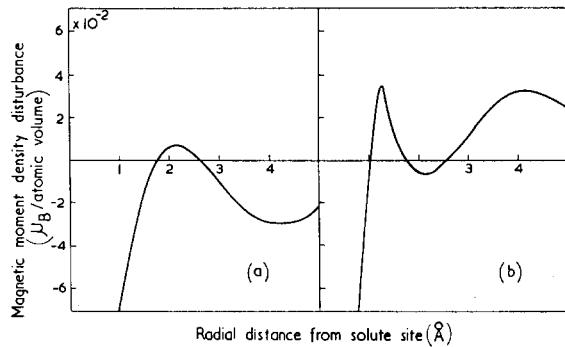


FIG. 3. Calculated magnetic-moment density disturbances at (a) a repulsive charge of one electron unit and (b) an attractive charge of similar size. These curves correspond to the simple model outlined in the text in which three electron gases are used to represent the electron bands in iron. The perturbing charges simulate transition-element solutes. In iron the total density of states at the Fermi level is dominated by the contribution from the majority spin-carrier d -electrons. Thus there is a loss of moment immediately at the site of a repulsive perturbing charge as shown in (a). The majority carrier d band is almost full, however, and it can make only a limited contribution to the screening of an attractive perturbing charge. Screening close to such a charge is, therefore, carried out largely by minority carriers and a loss of moment at the perturbing site again ensues as shown in (b).

Fermi vector. These three pairs of parameters are given values roughly consistent with the properties calculated by Wakoh and Yamashita⁴ for (a) the majority carrier d -hole Fermi surfaces, (b) the s -electron Fermi surface corresponding to the majority spin direction, and (c) the minority carrier surfaces. Numerical solutions are obtained for the screening around point charges. The calculations are self-consistent in the sense that the changes in electrostatic and exchange energies resulting from population-density changes in the gases are taken into account. For attractive perturbing charges the restriction is imposed that the population density of gas (a) above cannot increase by more than 0.15 electron per atomic volume. The results of such calculations for one electron unit each of attractive and repulsive point charge are shown in Fig. 3.

There is a rough qualitative correspondence between the forms of the magnetic disturbances plotted in Figs. 2 and 3, thus confirming that the crude model described above probably contains the essential physical features underlying the behavior of iron-transition-element alloys.

There are, of course, very considerable differences between the experimental and calculated curves. The radial scale of the curves in Fig. 3 is much contracted compared with that of the curves in Fig. 2. This it is thought, could well be the result of the use of a continuum model. Screening in a real crystal takes place as a result of charges induced in orbitals at atomic sites. In iron the nearest-neighbor distance is about 2.5 Å. Thus, apart from the impurity site itself, little screening is possible inside a radius of, say 2 Å. The continuum model, however, permits screening at all radii. A second

difference is the continuation in the curves in Fig. 3 of oscillations out to large radii. In a real crystal thermal and impurity scattering of electrons will lead to some damping of the long-range fluctuations. Also the marked oscillatory effects in the calculated curves may to some extent result from the use of a few simple spherical surfaces in place of the complex Fermi-surface structure of iron. On the other hand the neutron measurements on which the experimental plots are based are of low resolution so that the curves in Fig. 2 really represent the convolution of a magnetic disturbance with a resolution function having a width of some 2 Å. Thus, it may be that part of the difference between the calculated and experimental curves arises as a result of shortcomings in the latter.

B. Nontransition-Element Solutes

The spatial distribution of the magnetic-moment disturbance associated with six nontransition-element impurities in ferromagnetic iron has been examined by Holden, Comly and Low.⁷ The solutes studied were Al, Ga, Si, Ge, Sn and Sb. Of these Al produces the least perturbation at neighboring iron atoms and creates a defect which comes close to being a simple magnetic vacancy. The other five impurities also give rise to effects which approach this description. However, small disturbances extending some angstroms into the iron host are present in all cases and the magnetic moments on iron atoms situated 4 or 5 Å from the impurity always exceed the moment on pure iron by amounts of the order of a percent. This can be seen in Fig. 4 where curves of magnetic-moment density disturbance are

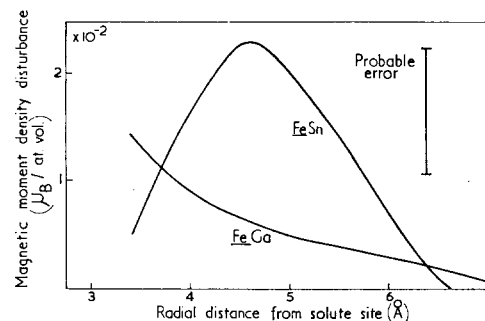


FIG. 4. The magnetic disturbances formed at nontransition-element solutes in iron approximate to magnetic vacancies. However, small magnetic perturbations are produced in the iron matrix and because of the large number of atoms affected these can give rise to considerable variation in the values of $d\mu/dc$. Examples derived from the neutron-scattering data of Holden, Comly, and Low⁷ of disturbances in magnetic-moment density in the iron matrix are shown in the figure. The effects are small, i.e., less than 1 or 2%, and as a consequence of this the fractional accuracy of the values for $\rho'(r)$ is low and the curves shown give only a very rough indication of the changes in the distribution of magnetic moment. In general nontransition-element solutes appear to increase the moment on iron atoms distant 4 or 5 Å from the impurity site.

⁷ T. M. Holden, J. B. Comly, and G. G. Low, Proc. Phys. Soc. (London) **92**, 726 (1967).

plotted for two representative solutes, Ga and Sn. Because the disturbances are small, the fractional errors in the experimental curves are large.

The neutron-scattering data for the six elements listed above are consistent with zero magnetic moment in d -states in the impurity cell.⁷ This means that variations among the values of $d\mu/dc$ observed are almost entirely attributable to the small magnetic disturbances in the iron host itself. Although these are only of the order of 1% per matrix atom, the large number of iron atoms affected by each impurity can lead to appreciable effects. Thus, while $d\mu/dc$ is about $-2.2 \mu_B$ for Al and Si, it is close to $-1.4 \mu_B$ for Ga.⁸

From the observations above it was concluded that the electrostatic screening of a nontransition-element impurity site is carried out by s and p electrons so that the electronic configuration of a solute atom is probably not greatly different from that of a free atom of the same element. The impurity s - and p -electron orbitals form resonating states with the d and s bands of the iron matrix. This leads to some electron scattering in the matrix and the small magnetic-moment perturbations observed. The sizes of the disturbances in the matrix do not appear to depend in any simple way on the properties of the solute site. Thus, the various values of $d\mu/dc$ observed are not directly related to the valence of the impurity atoms or to the magnetic-moment deficit at the impurity site (as the impurity moments are all close to zero, the moment deficit is approximately constant). Presumably the driving force for the perturbation must depend in some way on the details of the overlap and screening effects that exist between impurity wavefunctions and the orbitals of nearest-neighbor iron atoms.

3. NICKEL-BASED ALLOYS

A. Transition-Element Solute

The magnetic-moment disturbances at transition-metal solutes in nickel have been examined by Collins and Low^{1,2} (V, Cr, Mn, Fe) and by Comly, Holden and Low⁹ (Nb, Mo, Ru, Rh, W, Re). The magnetic defects formed are of two types. In one type (Mn, Fe, Rh) the magnetic disturbance is positive and confined to the impurity site. All the remaining solutes lead to a widespread loss of magnetic moment extending some 5 Å into the nickel matrix.

The magnetic behavior associated with the first group of impurities, Mn, Fe, Rh, (and, although not examined, almost certainly Co also), can be qualitatively understood in terms of simple band theory.¹⁰ The screening

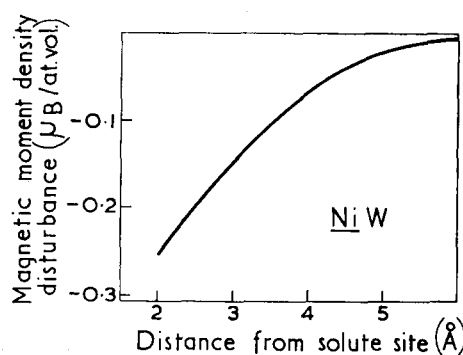


FIG. 5. The magnetic-moment disturbances observed in alloys of nickel containing transition-element solutes fall into two categories. Mn, Fe, Co and Rh produce an increase in moment which is confined to the impurity site. On the other hand the transition-metal solutes that cause departures from the Slater-Pauling curve give rise to losses of moment which are widespread in the nickel matrix. The example shown is based on the neutron-scattering measurements of Comly, Holden and Low⁹ and corresponds to Ni W.

of the change in core charge Δz at a solute atom is carried out by electrons from the minority carrier d band of nickel as the majority carrier band is virtually full. As Δz is negative, this leads to an increase of moment at the impurity site (1 Bohr magneton per electron subtracted) and gives agreement with the Slater-Pauling curve. The range of the magnetic disturbance is dependent on the electrostatic screening length of the d -electron gas in the minority carrier band. The density of states is high, and a short-range effect is therefore expected in agreement with the experimental result that the disturbances are located almost entirely within the impurity cell. Thus, both the magnitude and the spatial distribution for defects of this group are consistent with the simple discussion outlined.

The remaining solutes (V, Cr, Nb, Mo, Ru, W, Re) give rise to spatially extended losses of moment. An example of the form of the disturbance produced in the nickel matrix is shown in Fig. 5. Because of the large changes in moment density outside the impurity cell, these distributions appear to be of a qualitatively different nature to any of the magnetic defects discussed so far. The fractional losses in magnetic moment at nickel atoms which are nearest neighbors to an impurity are as high as 30%, i.e., $0.2 \mu_B/\text{atom}$. Even on an absolute scale this is three or four times the largest disturbance observed in an iron matrix.

So far in this paper all the discussion of magnetic disturbances has been in terms of electrostatic screening propagated through the band structure. This gives rise to disturbances of a few hundredths of a Bohr magneton per atomic volume at the nearest-neighbor sites. The large demagnetizations of the matrix observed in the present nickel alloys seem to require a distinct departure from this type of explanation and Friedel¹⁰ was the first to point out that a sufficiently large repulsive potential (Δz sufficiently negative) will produce bound-hole states above the d bands. The strength

⁸ A. T. Aldred, J. Appl. Phys. **37**, 1344 (1966).

⁹ J. B. Comly, T. M. Holden, and G. G. Low, (to be published in J. Physics C.).

¹⁰ J. Friedel, Nuovo Cimento (Suppl.) **7**, 287 (1958). For later work see J. Kanamori, J. Appl. Phys. **36**, 929 (1965); H. Hayakawa, Tech. Rept. A226 of Inst. Solid State Physics, University of Tokyo (1966) and Ref. 5.

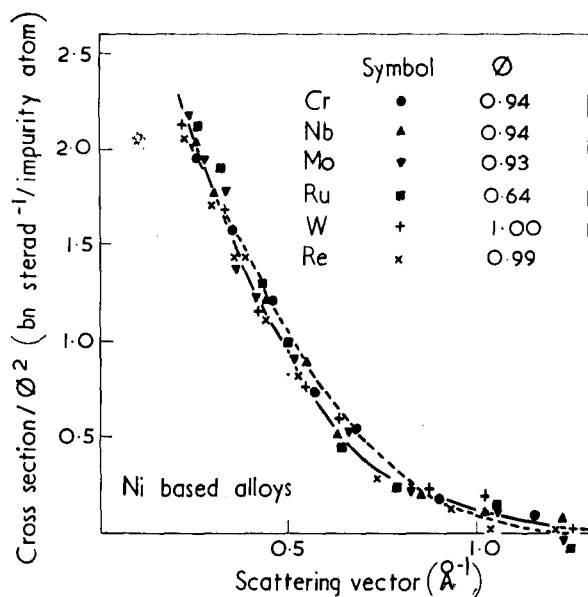


FIG. 6. Neutron cross sections of magnetic defect scattering from alloys of nickel containing dilute concentrations of transition-element solutes which cause departures from Slater-Pauling behavior. These data are from experiments by Collins and Low² and Comly, Holden and Low.⁹ The results for each impurity have been scaled relative to those of other elements so as to reduce all the cross sections to a common curve. The striking similarity in shape of the cross-section plots revealed in this way implies a corresponding similarity in the shape of the magnetic defects associated with the six solutes concerned. The dashed curve corresponds to scattering calculated from a model described in the text which leads to a defect shape roughly independent of magnitude as required by the experimental results.

of the perturbation caused by a solute atom depends both on Δz and on the transition series to which the solute belongs: thus the latter effect causes Fe and Ru to appear in different groups above. The bound states are of course formed at the expense of states in the d bands. To some extent the loss of d -band holes arising in this way is offset by the loss of $-\Delta z$ electrons from the d -bands necessary in the electrostatic screening of the impurity. Thus, if the bound-hole states are n -fold degenerate (including spin), $n + \Delta n = -\Delta n_h$ holes per impurity are lost from the d bands. Friedel assumed (i) that $n = 10$ so that $\Delta n_h = -(10 + \Delta z) = -n_v$, where n_v is the number of electrons outside of the outermost closed shell of a neutral atom of the impurity concerned, and (ii) that the energy splitting between the majority and minority spin d bands in the alloy is everywhere sufficient to maintain full occupation of the majority spin band. It follows on this model that $d\bar{\mu}/dc = \Delta n_h = -n_v$, which is in approximate agreement with experiment. Also implicit in this discussion is the assumption (iii) that the presence of the impurity causes no net interchange of populations between s and d bands and that changes in polarization effects in the s bands can be neglected.

The spatial distribution of the magnetization disturbance in this model appears to be dependent on the form

of the local bound-hole state. This in turn would be expected to depend on the impurity involved, so that the neutron-scattering form factor would vary from alloy to alloy. Recent neutron experiments⁹ force us to re-examine the details of these arguments concerning spatial distribution while retaining the basic assumption of bound-state formation. Figure 6 shows the cross sections for neutron scattering from six of the impurities listed above. The data for each element have been scaled relative to those of other elements with the result that they lie on the common solid curve shown. V alone of the solutes above shows a different form of cross section. The striking similarity in shape of the six cross sections shown in Fig. 6 implies a corresponding similarity in the shape of the defects responsible for the scattering. This, it is felt, is difficult to reconcile with the hypothesis that the form of the disturbances in the matrix is directly linked with the bound-state wavefunctions. The latter are expected to depend sensitively on Δz and on the transition series to which an impurity belongs.

In order to understand the similarity in defect shape implied by the data in Fig. 6 the following discussion has been offered.⁹ If we do not make assumptions (i), (ii), and (iii) above, we have that $d\bar{\mu}/dc = \Delta n_h = -(n + \Delta z + \Delta n_{\text{trans}})$. Here $\Delta n_{\text{trans}} = \Delta n_{sd} + 2\Delta n_{dd}$, where Δn_{sd} is the net number of electrons transferred from s to d bands owing to the presence of the impurity, and Δn_{dd} is the net number of holes created by the impurity in the majority spin d bands. Polarization effects in the s -bands are still neglected for simplicity, although it is by no means clear that they do not play a part in the magnetization changes. The suggested explanation of the experimental results is that the defects observed consist of a part (a) corresponding to $n + \Delta z$ above and a second part (b) corresponding to Δn_{trans} . Part (a) arises directly from the effects of the bound-hole states and electrostatic screening at the impurity and, as we have discussed, is probably sensitively dependent on Δz , etc., and thus varies both in form and magnitude from impurity to impurity. It is probable that part (a) is large and of importance only in the immediate neighborhood of the impurity. Part (b) may be regarded as the response of the matrix to the driving force embodied in part (a). Thus, part (a) will create a local demagnetization at the impurity as a result of which the surrounding matrix will suffer a partial loss of magnetization out to a range dependent on the properties of the matrix itself. The response of the matrix could be roughly expressed in terms of an integral equation in which the properties of the matrix are summarized as a nonlocal and nonlinear susceptibility, i.e.,

$$\rho(\mathbf{r}) = \int d\mathbf{r}' \chi(\mathbf{r}, \mathbf{r}') I\rho(\mathbf{r}'). \quad (2)$$

Here $\rho(\mathbf{r})$ is the magnetic moment density and $I\rho(\mathbf{r}')$

represents the exchange field at \mathbf{r}' in the molecular field approximation.

The magnitude and shape of the part (b) of the defect will depend both on part (a), which supplies the driving force, and on χ . However, if part (b) is spatially extensive compared with part (a), the shape of (b) will be largely determined by the properties of χ while its magnitude alone will derive from (a). This is the central point of the suggested explanation of the similarity in defect shape observed experimentally. It is proposed that as well as the part (a) effects envisaged by Friedel, additional part (b) demagnetization of the matrix also occurs. Furthermore it is assumed that the spatial range of (b) compared with (a) is large, so that the overall shape of the defect is mainly dependent on χ . If it is assumed that, except very close to the impurity, χ retains its pure matrix characteristics, we have a defect shape which is dependent on the matrix and only a weak function of the impurity concerned.

This suggested explanation has been illustrated by numerical calculations in terms of a simplified model based on Eq. (2). A driving force consisting of a d -hole decrease (from bound-state formation) is assumed to extend just to include the nearest-neighbor cells. For simplicity charge neutrality is assumed in the matrix (we noted above that departures from neutrality at nearest-neighbor positions and beyond lead only to magnetic effects small compared with those under discussion) and the effects described under Δn_{trans} above are limited to the transfer of electrons between d bands. Thus, in this approximation, $d\bar{\mu}/dc = -(n + \Delta z + 2\Delta n_{dd})$ where the electrostatic screening corresponding to Δz is confined to the impurity cell and the effects of the bound-state formation, denoted by n , are limited to within the outer boundaries of the nearest-neighbor cells. The properties of the susceptibility function used in Eq. (2) to find the magnitude and distribution of Δn_{dd} are made roughly consistent with the recently calculated density of states and exchange splitting of ferromagnetic nickel.¹¹ Fourier transformation of the calculated defects leads to scattering cross-section curves in good agreement with experiment. The adjustable parameter used to fit to the magnitude of the observed scattering is the d -hole loss, n . An example of a calculated cross section is shown as a dashed curve in Fig. 6.

In a summary, therefore, it is believed that the widespread losses of magnetic moment observed around those transition-element impurities in nickel which cause departures from the Slater-Pauling curve, are associated with bound impurity states as proposed by Friedel.¹⁰ However, it is suggested that the shape and spatial range of the defects do not reflect the extent of the bound-state wavefunctions. The form of the defects is mainly dependent on properties of the nickel matrix, which may be summarized in terms of a nonlocal

¹¹ L. Hodges, H. Ehrenreich, and N. D. Lang, Phys. Rev. **152**, 505 (1966).

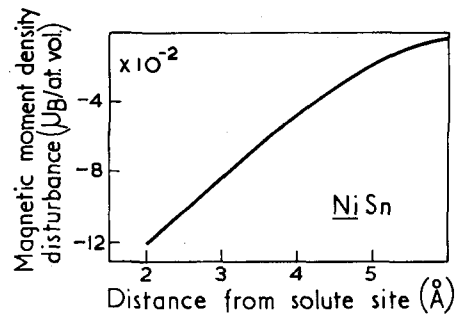


FIG. 7. Nontransition-element impurities in nickel lead to widespread losses of magnetic moment from the matrix. These disturbances are of a similar shape to the defect shown in Fig. 4 in connection with transition-metal alloys which depart from the Slater-Pauling curve. However, the disturbances for the nontransition elements are in general smaller than those for transition elements. An example (NiSn) taken from the experimental results of Comly, Holden and Low⁹ is shown in the figure.

susceptibility function. The bound states provide a driving force creating a local disturbance which is propagated outwards, in a manner determined by the susceptibility, to form the extended defects observed.

B. Nontransition-Element Solutes

The scattering from seven nontransition-element solutes (Zn, Al, Ga, Si, Ge, Sn, Sb) in nickel has also been examined by Comly, Holden and Low.⁹ These impurities all give rise to losses of magnetic moment from the surrounding nickel matrix of much the same form as those associated with the transition-element impurities just discussed. As an example, the defect for Sn in nickel is shown in Fig. 7. On the whole the magnitudes of the defects at the nontransition-element solutes are smaller than those at the transition-metal impurities, there being a rough proportionality with n_v , the number of electrons outside the outermost closed shell of a neutral atom of the solute concerned.

There does not appear to be any simple explanation for the defects observed in the nontransition-element alloys. Their considerable extension into the nickel matrix precludes any direct link between electrostatic screening charge and magnetic disturbance. Thus, it seems probable that the screening will be carried out largely within the impurity cell by s and p electrons so that the electronic constitution of an impurity in the nickel matrix is quite similar to that of a free atom of the same element. The fact that the present defects are similar in shape to those discussed in the last section in connection with transition-element solutes suggests that both sets are dependent on the same mechanism for their formation. The driving force in the present case need not be a loss of holes as it was for the transition-element solutes. Other magnetic disturbances close to an impurity would be propagated out in much the same way. One possibility is a diminution in exchange strength in the vicinity of a nontransition element

through the mechanism suggested by Beeby.¹² His proposal involves screening of the impurity by s and p electrons which are to some extent mixed into the d band. As a result of this admixture the band wavefunctions are more spread out around the lattice positions with a consequent reduction in electron-electron interactions.

4. CONCLUSIONS

The information obtained by recent measurements of the elastic magnetic diffuse neutron scattering from iron- and nickel-based alloys containing small additions of both transition and nontransition-element solutes is summarized. The experimental data lead to plots of the disturbance in magnetic-moment density near an impurity. In the case of transition-metal solutes in iron, the type of defect observed shows a marked correlation with whether the impurity lies to the left or to the right of iron in the periodic table. This suggests that the magnetic disturbances are associated with charge screening in the electron bands and a simple model based on this assumption gives qualitative agreement with the observed defect shapes. Nontransition-element impurities

in iron create disturbances which approximate to magnetic vacancies. Nickel alloys show magnetic defects of two kinds. Some transition-element solutes such as Mn, Fe, Co, Rh, give rise to large increases in moment which are confined to the impurity cell. This behavior can also be understood in terms of charge screening, in this case by minority spin carriers as the nickel majority carrier band has little or no Fermi surface. Other impurities in nickel, e.g., Cr and Al, lead to widespread losses of magnetic moment from the matrix material surrounding the solute site. In the case of transition-element impurities these defects are associated with the formation of bound states above the band. A defect mechanism is proposed in which the extent of a defect does not depend directly on the range of the bound-state wavefunctions.

ACKNOWLEDGMENTS

The work described above is the result of collaboration between the present author and Drs. M. F. Collins, J. B. Comly, and T. M. Holden. The interpretation of the experimental results owes a very great deal to guidance from Dr. W. M. Lomer which is gratefully acknowledged. M. Agrell is thanked for his help with numerical calculations.

¹² J. L. Beeby, Phys. Rev. **141**, 781 (1966).

Spin Impurities in Heisenberg Antiferromagnets

L. R. WALKER

Bell Telephone Laboratories, Inc., Murray Hill, New Jersey

Work on the effects produced by a single spin impurity placed in a uniform spin system which interacts through Heisenberg exchange and with anisotropy fields is considered. The problem is formulated in terms of a two-time Green's function, whose equation of motion is simplified by the rpa. An infinite set of equations arises which contains the spin magnetizations as parameters; these are to be found consistently in terms of the Green's functions using the Callen-Shtrikman algorithm. At low temperatures an approximation equivalent to that of spin-wave theory reduces the set of equations to nine in the bcc case. These may be solved and permit a discussion of the modes of excitation of the impurity host system. These may be localized, above or below the spin-wave band, or act as resonant modes within it. Explicit expressions for the spin deviation at any site may also be given. Exactly similar equations may be used at higher temperatures if it is assumed that in the equations all spins save the impurity have the same magnetization. The impurity magnetization itself may be found by solving iteratively the equations for the impurity Green's function and the magnetization. This model is very useful for general qualitative discussions. Magnetization vs. temperature curves have recently been obtained (with D. Hone and H. E. Callen) for various impurity situations, using a method previously applied by the same authors to ferromagnetic hosts. This model determines only the impurity magnetization, but the first shell of down-spins is allowed to depart from the host magnetization, although it is only treated approximately. Self-consistency is achieved, however, for the impurity. The convergence is excellent. Some vigilance has to be exercised in searching for localized modes and in doing integrations over the sharp peaks which may occur in the Green's functions. Examples of magnetization curves are given for systems with resonant modes, with localized modes above and below the spin wave band, with levels which change from resonant to localized as the temperature changes and so forth. In the absence of anisotropy, some of the features of the zero-point deviation of the impurity which appear may be predicted by the use of second-order perturbation theory treating the transverse exchange as a perturbation.